ICAS PAPER No. 72 – 28

DYNAMIC INELASTIC PROPERTIES OF MATERIALS
Part I – Damping Characteristics of Fiber Composites
Part II – Representation of Time Dependent Characteristics of Metals

by
Z. Hashin, S. R. Bodner and Y. Partom
Department of Materials Engineering
Technion, Israel Institute of Technology
Haifa, Israel

The Eighth Congress of the International Council of the Aeronautical Sciences

INTERNATIONAAL CONGRESCENTRUM RAI–AMSTERDAM, THE NETHERLANDS
AUGUST 28 TO SEPTEMBER 2, 1972

Price: 3. Dfl.

DYNAMIC INELASTIC PROPERTIES OF MATERIALS

Part I - Damping Characteristics of Fiber Composites(*)

Zvi Hashin
Department of Materials Engineering
Technion - Israel Institute of Technology
Haifa, Israel

Abstract

Analytical results for complex moduli of uniaxially fiber reinforced materials made of viscoelastic matrix and elastic fibers are reviewed. A general method is established to predict complex moduli and loss tangents of viscoelastic laminates made of uniaxially reinforced laminae. Results are used to analyze some simple cases of vibrations of structures made of such viscoelastic composites.

1. Introduction

The ever increasing use of fiber composites for aero/space structures requires the development of rational methods for prediction of their relevant properties within engineering accuracy.

In most current fiber composites the matrix is a polymer such as epoxy. It is well known that such polymers exhibit the effect of vibration damping. Therefore such damping effects will also occur in composites in which the matrix is polymeric. Since aero/space structures are subjected to severe vibrational environment and since vibration damping is beneficial, the quantitative prediction of such damping is of considerable engineering importance.

It is of interest to emphasize the unique combination of desirable properties which are exhibited by fiber composites: Superior strength and stiffness, low weight and vibration damping. No other materials seem to possess this many advantages.

In order to handle the problem analytically, it is assumed that the matrix is linearly viscoelastic. Its dynamic viscoelastic properties can then be characterized in terms of the usual complex moduli of viscoelasticity which are assumed to be known on the basis of experiments. The fibers are represented as linear elastic. The composite with such constituents behaves macroscopically as a linear viscoelastic body which is characterized by effective complex moduli. There arise three classes of important investigation:

(a) Prediction of effective complex moduli of a uniaxially reinforced material on the basis of matrix complex moduli; fiber elastic moduli and internal geometrical parameters such as constituent volume fractions, fiber shapes, etc.

(b) Prediction of the effective complex moduli of a laminate, whose laminae are composed of uniaxially reinforced material, on the basis of the uniaxial material effective complex moduli found in (a) and the laminate internal geometry.

(c) Viscoelastic vibration analysis of structures made of fiber composites.

These different kinds of problems will be discussed consecutively.

2. Complex Moduli of Uniaxially Fiber Reinforced Materials

A general theory of prediction of effective complex moduli of composites with linear viscoelastic constituents has been given previously[1,2,3]. It will here suffice to discuss without proof some results which are pertinent for the present investigation.

Let the local average strains and stresses in a composite be of oscillatory nature. Thus:

$$\bar{\varepsilon}_{ij} = \tilde{\varepsilon}_{ij}\, e^{\imath\omega t}$$
$$\bar{\sigma}_{ij} = \tilde{\sigma}_{ij}\, e^{\imath\omega t} \tag{2.1}$$

where overbars denote average, $\imath = \sqrt{-1}$, ω is frequency, t is time and latin subscripts range over 1,2,3. The effective complex moduli $\tilde{C}^*_{ijk\ell}$ of a generally anisotropic composite are defined by the relation:

$$\tilde{\sigma}_{ij} = \tilde{C}^*_{ijk\ell}(\imath\omega)\, \tilde{\varepsilon}_{k\ell} \tag{a}$$
$$\tilde{C}^*_{ijk\ell}(\imath\omega) = C^{*R}_{ijk\ell}(\omega) + \imath\, C^{*I}_{ijk\ell}(\omega) \tag{b}$$

(2.2)

where superscripts R and I denote real and imaginary parts respectively.

The assumption is made that the fiber reinforced material under consideration is macroscopically transversely isotropic with respect to fiber direction. Then (2.2a) assumes the form:

$$\tilde{\sigma}_{11} = \tilde{C}_{11}\,\tilde{\varepsilon}_{11} + \tilde{C}_{12}\,\tilde{\varepsilon}_{22} + \tilde{C}_{12}\,\tilde{\varepsilon}_{33}$$
$$\tilde{\sigma}_{22} = \tilde{C}_{12}\,\tilde{\varepsilon}_{11} + \tilde{C}_{22}\,\tilde{\varepsilon}_{22} + \tilde{C}_{23}\,\tilde{\varepsilon}_{33}$$
$$\tilde{\sigma}_{33} = \tilde{C}_{12}\,\tilde{\varepsilon}_{11} + \tilde{C}_{23}\,\tilde{\varepsilon}_{22} + \tilde{C}_{22}\,\tilde{\varepsilon}_{33}$$
$$\tilde{\sigma}_{12} = 2\tilde{C}_{44}\,\tilde{\varepsilon}_{12}$$
$$\tilde{\sigma}_{23} = (\tilde{C}_{22} - \tilde{C}_{23})\,\tilde{\varepsilon}_{23}$$
$$\tilde{\sigma}_{31} = 2\tilde{C}_{44}\,\tilde{\varepsilon}_{31} \tag{2.3}$$

(*) Supported by the Air Force Office of Scientific Research under Contract F 44620-71-C-0100 through the European Office of Aerospace Research (EOAR), U.S. Air Force.

where x_1 is in fiber direction and x_2, x_3 are in the transverse plane, Fig. 1.

In another notation, the complex moduli in (2.3) are written:

$$\begin{aligned} \tilde{C}_{11} &= \tilde{n} \\ \tilde{C}_{12} &= \tilde{\ell} \\ \tilde{C}_{22} &= \tilde{k} + \tilde{G}_T \\ \tilde{C}_{23} &= \tilde{k} - \tilde{G}_T \\ \tilde{C}_{44} &= \tilde{G}_A \end{aligned} \tag{2.4}$$

Here $\tilde{k}$ is a transverse complex bulk modulus, $\tilde{G}_T$ - transverse complex shear modulus in x_2, x_3 plane and $\tilde{G}_A$ - axial complex shear modulus in planes containing fiber direction x_1. The physical interpretation of $\tilde{n}$ and $\tilde{\ell}$ is here of little interest.

Inversion of (2.3) is written in the form:

$$\begin{aligned} \tilde{\varepsilon}_{11} &= \frac{1}{\tilde{E}_A}\tilde{\sigma}_{11} - \frac{\tilde{\nu}_A}{\tilde{E}_A}\tilde{\sigma}_{22} - \frac{\tilde{\nu}_A}{\tilde{E}_A}\tilde{\sigma}_{33} \\ \tilde{\varepsilon}_{22} &= -\frac{\tilde{\nu}_A}{\tilde{E}_A}\tilde{\sigma}_{11} + \frac{1}{\tilde{E}_T}\tilde{\sigma}_{22} - \frac{\tilde{\nu}_T}{\tilde{E}_T}\tilde{\sigma}_{33} \\ \tilde{\varepsilon}_{33} &= -\frac{\tilde{\nu}_A}{\tilde{E}_A}\tilde{\sigma}_{11} - \frac{\tilde{\nu}_T}{\tilde{E}_T}\tilde{\sigma}_{22} + \frac{1}{\tilde{E}_T}\tilde{\sigma}_{33} \\ \tilde{\varepsilon}_{12} &= \frac{\tilde{\sigma}_{12}}{2\tilde{G}_A} \\ \tilde{\varepsilon}_{23} &= \frac{\tilde{\sigma}_{23}}{2\tilde{G}_T} \\ \tilde{\varepsilon}_{31} &= \frac{\tilde{\sigma}_{31}}{2\tilde{G}_A} \end{aligned} \tag{2.5}$$

where $\tilde{E}_A$ and $\tilde{E}_T$ are complex Youngs' moduli in axial (fiber) direction and transverse (to fiber) direction, respectively, and $\tilde{\nu}_A$ and $\tilde{\nu}_T$ are associated complex Poisson's ratios.

Establishment of analytical expressions for the various effective complex moduli listed above in terms of matrix complex moduli, fiber elastic moduli and phase geometry is based on a correspondence principle[1,2] which states: The effective complex moduli of a viscoelastic composite are obtained by replacement of phase elastic moduli by phase complex moduli in the expressions for the effective elastic moduli of a composite with identical phase geometry.

In the usual fiber reinforced materials the following conditions are usually fulfilled with sufficient accuracy

(a) Fibers are by an order of magnitude stiffer than matrix

(b) The matrix is isotropic and is viscoelastic in shear only

(c) The matrix shear loss tangent is not larger than 0.1. Thus:

$$\tan \delta_G^m = \frac{G_m^I}{G_m^R} \leq 0.1 \tag{2.6}$$

Under these conditions the following results have been shown[3] to be valid.

(d) The imaginary parts of the effective complex moduli, $\tilde{n}$, $\tilde{I}$, $\tilde{k}$, $\tilde{E}_A$ are much smaller than the imaginary parts of the effective shear moduli $\tilde{G}_A$, $\tilde{G}_T$ and of $\tilde{E}_T$.

(e) To obtain real parts of all effective complex moduli it is merely necessary to take corresponding expressions for effective elastic moduli and to replace in them matrix elastic moduli by real parts of matrix complex moduli.

Some simple general results which are valid under the conditions listed above will now be given:

For uniaxial stressing in fiber direction

$$\begin{aligned} \tilde{E}_A(\imath\omega) &= \tilde{E}_m(\imath\omega)\, v_m + E_f\, v_f \\ E_A^R(\omega) &= E_m^R(\omega)\, v_m + E_f\, v_f \\ E_A^I(\omega) &= E_m^I(\omega)\, v_m \\ \tan \delta_E &= \frac{E_A^I}{E_A^R} = \frac{\tan \delta_E^m}{1 + E_f v_f / E_m^R v_m} \ll \tan \delta_E^m \end{aligned} \tag{2.7}$$

Here m and f denote matrix and fibers, respectively, and v stands for volume fraction, $\tan \delta_E$ is the loss tangent for uniaxial stressing in fiber direction while $\tan \delta_E^m$ is the corresponding loss tangent for the isotropic matrix.

For axial shear

$$\begin{aligned} \tilde{G}_A(\imath\omega) &= \tilde{G}_m(\imath\omega)\,\frac{1 + v_f}{1 - v_f} \\ G_A^R(\omega) &= G_m^R\,\frac{1 + v_f}{1 - v_f} \\ G_A^I(\omega) &= G_m^I\,\frac{1 + v_f}{1 - v_f} \\ \tan \delta_{G_A} &= \tan \delta_G^m \end{aligned} \tag{2.8}$$

For transverse shear

$$G_T^I \cong G_T^R \tan \delta_G^m$$

$$\tan \delta_{G_T} = \tan \delta_G^m \tag{2.9}$$

An expression for G_T^R has been given in [2,3]. Results for other complex moduli may also be found in these references.

3. Complex Moduli of Laminates

The laminates to be considered are composed of plane laminae of uniaxially fiber reinforced materials, the direction of reinforcement being different in each lamina. The laminate is referred to a fixed coordinate system x_1, x_2, x_3 where x_1, x_2 are in the plane of the laminae and x_3 is normal to it, Fig. 2. The nth lamina in the laminate is referred to a material system of axes $x_1^{(n)}$, $x_2^{(n)}$, x_3 where $x_1^{(n)}$ is in fiber direction, $x_2^{(n)}$ is normal to the fibers and x_3 coincides with the laminate x_3. The position of the $x_1^{(n)}$, $x_2^{(n)}$ system is defined with respect to the x_1, x_2 system by the reinforcement angle

$$\theta_n = \sphericalangle (x_1^{(n)}, x_1) \tag{3.1}$$

Fundamental assumptions of fiber composite laminate theory are: (a) Any lamina can be replaced by a homogenous material whose properties are the effective properties of the uniaxial FRM of which the lamina is made. (b) The laminae are in states of plane stress.

First an elastic laminate will be considered. The plane stress-strain relations of a lamina referred to its material system of axes $x_1(n)$, $x_2(n)$ are then:

$$\begin{aligned}
\varepsilon_{11}^{(n)} &= \frac{1}{E_A}\sigma_{11}^{(n)} - \frac{\nu_A}{E_A}\sigma_{22}^{(n)} \\
\varepsilon_{22}^{(n)} &= -\frac{\nu_A}{E_A}\sigma_{11}^{(n)} + \frac{1}{E_T}\sigma_{22}^{(n)} \\
\varepsilon_{12}^{(n)} &= \frac{\sigma_{12}^{(n)}}{2G_A}
\end{aligned} \tag{3.2}$$

where:

E_A - axial Youngs modulus (in fiber direction)

ν_A - associated axial Poisson's ratio

E_T - transverse Youngs modulus (normal to fibers)

G_A - axial shear modulus (in $x_1^{(n)}$, $x_2^{(n)}$ plane)

The inverse of (3.2) is:

$$\begin{aligned}
\sigma_{11}^{(n)} &= C_{11}\,\varepsilon_{11}^{(n)} + C_{12}\,\varepsilon_{22}^{(n)} \\
\sigma_{22}^{(n)} &= C_{12}\,\varepsilon_{11}^{(n)} + C_{22}\,\varepsilon_{22}^{(n)} \\
\sigma_{12}^{(n)} &= 2C_{44}\,\varepsilon_{12}^{(n)}
\end{aligned} \tag{3.3}$$

where:

$$\begin{aligned}
C_{11} = C_{1111} &= \frac{E_A}{1 - \frac{E_A}{E_T}\nu_A^2} \\
C_{12} = C_{1122} &= \frac{\nu_A E_T}{1 - \frac{E_A}{E_T}\nu_A^2} \\
C_{22} = C_{2222} &= \frac{E_T}{1 - \frac{E_A}{E_T}\nu_A^2} \\
C_{44} = C_{1212} &= G_A
\end{aligned} \tag{3.4}$$

In terms of the four index moduli in (3.4), (3.3) can be written compactly as:

$$\sigma_{\alpha\beta}^{(n)} = C_{\alpha\beta\gamma\delta}\,\varepsilon_{\gamma\delta}^{(n)} \tag{3.5}$$

where here and from now on Greek indices range over 1,2.

For the sake of simplicity there will be considered the special group of laminates in which the application of membrane force $N_{\alpha\beta}$ in the plane of the laminate does not induce bending or torsion in the laminae. The most important kind of laminate which fulfills this requirement is a symmetric laminate. Such a laminate has the property that its middle plane is a plane of symmetry for the geometric and elastic moduli of the laminate. The laminate is thus composed of laminae pairs in each of which the laminae are of same thickness, are symmetrically located with respect to the middle plane and have the same elastic properties with respect to the x_1, x_2 system.

The last condition is most commonly fulfilled by laminae made of identical material and same reinforcement angle θ_n (3.1), in each pair. The elastic stress-strain relation of such a laminate is given by

$$\begin{aligned}
\overline{\sigma}_{\alpha\beta} &= \frac{N_{\alpha\beta}}{h} = C^*_{\alpha\beta\gamma\delta}\overline{\varepsilon}_{\gamma\delta} \quad (a) \\
C^*_{\alpha\beta\gamma\delta} &= \sum_{n=1}^{N} {}^{(n)}C_{\alpha\beta\gamma\delta}\, t_n/h \quad (b)
\end{aligned} \tag{3.6}$$

where

$\bar{\sigma}_{\alpha\beta}$ - applied average plane stress

$\bar{\varepsilon}_{\alpha\beta}$ - average strain

h - laminate thickness

$C^*_{\alpha\beta\gamma\delta}$ - effective elastic moduli of laminate

t_n - thickness of n^{th} lamina

N - number of laminae

$^{(n)}C_{\alpha\beta\gamma\delta}$ - the laminae elastic moduli (3.4) transformed to the x_1, x_2 system of axes.

For establishment of the result (3.6) see e.g.[4]. Proof that (3.6) is based on an elasticity solution which is exact in the Saint Venant sense for a laminate whose thickness is small compared to its plane dimensions has been given by B.W. Rosen (unpublished).

Let it be now assumed that the laminate is viscoelastic but remains symmetric as described above. The laminate is subjected to oscillatory membrane loads

$$N_{\alpha\beta} = \tilde{N}_{\alpha\beta}\, e^{i\omega t} \tag{3.7}$$

The average stresses associated with (3.7) are then:

$$\bar{\sigma}_{\alpha\beta} = \frac{N_{\alpha\beta}}{h} = \frac{\tilde{N}_{\alpha\beta}}{h}\, e^{i\omega t} = \tilde{\bar{\sigma}}_{\alpha\beta}\, e^{i\omega t} \tag{3.8}$$

The strain response of the laminate is

$$\bar{\varepsilon}_{\alpha\beta} = \tilde{\bar{\varepsilon}}_{\alpha\beta}\, e^{i\omega t} \tag{3.9}$$

The relation between $\tilde{\bar{\sigma}}_{\alpha\beta}$ and $\tilde{\bar{\varepsilon}}_{\alpha\beta}$ is written:

$$\tilde{\bar{\sigma}}_{\alpha\beta} = \tilde{C}^*_{\alpha\beta\gamma\delta}\,(i\omega)\,\tilde{\bar{\varepsilon}}_{\gamma\delta} \tag{3.10}$$

where $\tilde{C}^*_{\alpha\beta\gamma\delta}$ are the effective complex moduli of the laminate.

It follows by the general correspondence principle of [1] which was quoted above that $\bar{C}^*_{\alpha\beta\gamma\delta}$ can be expressed in form (3.6b). Thus:

$$\tilde{C}^*_{\alpha\beta\gamma\delta}\,(i\omega) = \sum_{n=1}^{N} {}^{(n)}\tilde{C}_{\alpha\beta\gamma\delta}\,(i\omega)\, t_n/h \tag{3.11}$$

The single laminae complex moduli $^{(n)}\tilde{C}_{\alpha\beta\gamma\delta}$ in (3.11) are interpreted as follows: In the material axes $x_1^{(n)}$, $x_2^{(n)}$ of the nth lamina the stresses and strains are:

$$\sigma^{(n)}_{\alpha\beta} = \tilde{\sigma}^{(n)}_{\alpha\beta} e^{i\omega t}$$
$$\varepsilon^{(n)}_{\alpha\beta} = \tilde{\varepsilon}^{(n)}_{\alpha\beta}\, e^{i\omega t} \tag{3.12}$$

The relation between $\tilde{\sigma}^{(n)}_{\alpha\beta}$ and $\tilde{\varepsilon}^{(n)}_{\alpha\beta}$ in (3.12) is of type (3.3-3.4). Thus:

$$\tilde{\sigma}^{(n)}_{\alpha\beta} = \tilde{C}_{\alpha\beta\gamma\delta}\,\tilde{\varepsilon}^{(n)}_{\gamma\delta} \tag{3.13}$$

$$C_{1111} = \tilde{C}_{11} = \frac{\tilde{E}_A}{1 - \frac{\tilde{E}_T}{\tilde{E}_A}\tilde{\nu}_A^2}$$

$$\tilde{C}_{1122} = \tilde{C}_{12} = \frac{\tilde{\nu}_A \tilde{E}_T}{1 - \frac{\tilde{E}_T}{\tilde{E}_A}\tilde{\nu}_A^2} \tag{3.14}$$

$$\tilde{C}_{2222} = \tilde{C}_{22} = \frac{\tilde{E}_T}{1 - \frac{\tilde{E}_T}{\tilde{E}_A}\tilde{\nu}_A^2}$$

$$\tilde{C}_{1212} = \tilde{C}_{44} = \tilde{G}_A$$

where $\tilde{E}_A$, $\tilde{E}_T$, $\tilde{\nu}_A$ and $\tilde{G}_A$ are the effective complex moduli of the uniaxial material which were discussed in par. 2.

If the complex stress strain relation (3.13) is transformed to the laminate axes x_1, x_2 it assumes the form:

$$^{(n)}\tilde{\sigma}_{\alpha\beta} = {}^{(n)}C_{\alpha\beta\gamma\delta}\,{}^{(n)}\tilde{\varepsilon}_{\gamma\delta}$$

This defines the $^{(n)}C_{\alpha\beta\gamma\delta}$ in (3.11).

By tensor transformation:

$$\begin{aligned}
{}^{(n)}\tilde{C}_{1111} &= {}^{(n)}\tilde{C}_{11} = \tilde{C}_{11}\cos^4\theta_n + \tilde{C}_{22}\sin^4\theta_n + \\
&+ 2\tilde{C}_{12}\cos^2\theta_n\sin^2\theta_n + 4\tilde{C}_{44}\cos^2\theta_n\sin^2\theta_n \\
{}^{(n)}\tilde{C}_{1122} &= {}^{(n)}\tilde{C}_{12} = (\tilde{C}_{11} + \tilde{C}_{22})\cos^2\theta_n\sin^2\theta_n + \\
&+\tilde{C}_{12}(\cos^4\theta_n + \sin^4\theta_n) - 4\tilde{C}_{44}\cos^2\theta_n\sin^2\theta_n \\
{}^{(n)}\tilde{C}_{2222} &= {}^{(n)}\tilde{C}_{22} = \tilde{C}_{11}\sin^4\theta_n + \tilde{C}_{22}\cos^4\theta_n + \\
&+ 2\tilde{C}_{12}\cos^2\theta_n\sin^2\theta_n + 4\tilde{C}_{44}\cos^2\theta_n\sin^2\theta_n
\end{aligned} \tag{3.16}$$

$$\begin{aligned}
{}^{(n)}\tilde{C}_{1112} &= {}^{(n)}\tilde{C}_{14} = -\tilde{C}_{11}\cos^3\theta_n\sin\theta_n + \\
&+ \tilde{C}_{22}\cos\theta_n\sin^3\theta_n + \tilde{C}_{12}(\cos^3\theta_n\sin\theta_n - \cos\theta_n\sin^3\theta_n) + \\
&+ 2\tilde{C}_{44}(\cos^3\theta_n\sin\theta_n - \cos\theta_n\sin^3\theta_n)
\end{aligned}$$

$$ {}^{(n)}\tilde{C}_{2212} = {}^{(n)}\tilde{C}_{24} = -\tilde{C}_{11}\cos\theta_n\sin^3\theta_n + \qquad (3.16 \text{ cont'd.}) $$

$$ + \tilde{C}_{22}\cos^3\theta_n\sin\theta_n + \tilde{C}_{12}(\cos\theta_n\sin^3\theta_n - \cos^3\theta_n\sin\theta_n) + $$

$$ + 2\tilde{C}_{44}(\cos\theta_n\sin^3\theta_n - \cos^3\theta_n\sin\theta_n) $$

$$ {}^{(n)}\tilde{C}_{1212} = {}^{(n)}\tilde{C}_{44} = (\tilde{C}_{11} + \tilde{C}_{22})\cos^2\theta_n\sin^2\theta_n - $$

$$ - 2\tilde{C}_{12}\cos^2\theta_n\sin^2\theta_n + \tilde{C}_{44}(\cos^2\theta_n - \sin^2\theta_n)^2 $$

The preceding developments together with the results for complex moduli of uniaxially fiber reinforced materials define the computation methods of the effective complex moduli of symmetric laminates as expressed by (3.11).

For practical purposes it is frequently necessary to compute the effective complex compliances which are defined as the inverse of (3.11). In matrix notation:

$$ \underline{\tilde{C}}^* \cdot \underline{\tilde{S}}^* = \underline{J} \qquad (3.17) $$

where $\underline{\tilde{S}}^*$ denotes the effective complex compliance matrix and $\underline{J}$ is the unit matrix. Separation of (3.17) into real and imaginary parts yields

$$ \underline{C}^{*R} \cdot \underline{S}^{*R} - \underline{C}^{*I} \cdot \underline{S}^{*I} = \underline{J} \qquad \text{(a)} $$

$$ \underline{C}^{*R} \cdot \underline{S}^{*I} - \underline{C}^{*I} \cdot \underline{S}^{*R} = 0 \qquad \text{(b)} \qquad (3.18) $$

Great facilitation is achieved if it is noted that in view of (2.6) the second term in the left side of (3.18a) can be neglected with respect to the first. It then follows:

$$ \underline{C}^{*R} \cdot \underline{S}^{*I} = \underline{J} \qquad \text{(a)} $$

$$ \underline{S}^{*I} = -\underline{S}^{*R} \cdot \underline{C}^{*I} \cdot \underline{S}^{*R} \qquad \text{(b)} \qquad (3.19) $$

Thus, once $\underline{C}^{*R}$ AND $\underline{C}^{*I}$ have been computed from (3.11), (3.19) define the effective complex compliance matrix by simple real matrix operations.

Another important simplification is obtained if in the laminate to each pair with reinforcement angle θ_n and thickness t_n corresponds another pair with reinforcement $-\theta_n$ and same thickness t_n. It is then easily realized by the form of (3.16) that all contributions to (3.11) of terms with odd powers of $\cos\theta_n$ and $\sin\theta_n$ cancel mutually. Thus in this event the effective complex moduli matrix (3.11) has the form

$$ \underline{\tilde{C}}^* = \begin{bmatrix} \tilde{C}^*_{1111} & \tilde{C}^*_{1122} & 0 \\ \tilde{C}^*_{1122} & \tilde{C}^*_{2222} & 0 \\ 0 & 0 & \tilde{C}^*_{1212} \end{bmatrix} = \begin{bmatrix} \tilde{C}^*_{11} & \tilde{C}^*_{12} & 0 \\ \tilde{C}^*_{12} & \tilde{C}^*_{22} & 0 \\ 0 & 0 & \tilde{C}^*_{44} \end{bmatrix} \qquad (3.20) $$

and so the laminate is macroscopically orthotropic. The situation just described is of frequent practical occurrence. For example a symmetric laminate with laminae reinforcement in $\theta_n = 0, 90°, \pm 45°$ directions.

4. Structural Applications

4.1 Free flexural vibrations of a fiber reinforced beam.

As a first example there is considered the case of free flexural vibrations of a simply supported beam which is uniaxially reinforced in beam axis direction. The purpose of the investigation is to compare vibration damping due to matrix viscoelasticity on the basis of the usual theory which neglects the effect of shear and on the basis of the more refined Timoshenko theory which takes into account shear as well as rotatory inertia. For isotropic materials, in which the complex Young's modulus loss tangent and the complex shear modulus loss tangent are of same order, the added effect of shear and rotatory inertia is small for vibration modes of low order and for long beams. In the present case, however, where the axial Young's modulus loss tangent is by an order of magnitude smaller than that of the axial shear modulus (section 2) the situation is quite different as will be shown below:

Considering only the effect of flexure the differential equation of the freely vibrating beam is:

$$ c^2 \frac{\partial^2 w}{\partial x^4} + \frac{\partial^2 w}{\partial t^2} = 0 \qquad \text{(a)} $$

$$ c^2 = \frac{\tilde{E}_A I}{\rho A} \qquad \text{(b)} \qquad (4.1) $$

where:

$\tilde{E}_A$ - complex axial Young's modulus

I - moment of inertia

A - area of cross section

ρ - density

Boundary conditions of free support are:

$$ w, \frac{\partial^2 w}{\partial x^2} = 0 \qquad x = 0, \ell \qquad (4.2) $$

Conventional viscoelastic vibrations analysis shows that the modes of vibration are given by

$$ w_n(x,t) = A_n \sin\frac{n\pi x}{\ell}\, e^{-\frac{1}{2}\omega_n^R \tan\delta_E t} e^{i\omega_n^R t} $$

where A_n is an arbitrary constant and

$$ \omega_n^R = \frac{n^2\pi^2}{\ell^2}\sqrt{\frac{E_A^R I}{\rho A}} \qquad \text{(a)} $$

$$ \tan\delta_E = \frac{\tan\delta_E^m}{1 + \frac{E_f^R v_f}{E_m^R v_m}} \qquad \text{(b)} \qquad (4.4) $$

Equ. (4.4b) is a repetition of (2.7d). The results are valid for small enough loss tangents, of order (2.6). The attenuation η_n is defined by

$$\eta_n = -\frac{\omega_n^R}{2}\tan\delta_E \tag{4.5}$$

Next the same beam is considered in Timoshenko fashion, with shear and rotatory inertia. By the correspondence principle for viscoelastic vibrations[5], the elastic Timoshenko beam equation[6] transforms into

$$c^2\frac{\partial^4 w}{\partial x^4} + \frac{\partial^2 w}{\partial t^2} - r^2\left(1 + \frac{k\tilde{E}_A}{\tilde{G}_A}\right)\frac{\partial^4 w}{\partial x^2 \partial t^2} + \frac{kr^2\rho}{\tilde{G}_A}\frac{\partial^4 w}{\partial t^4} = 0 \tag{4.6}$$

where c^2 is given by (4.1b), $\tilde{G}_A$ is the axial complex shear modulus (2.8a), k is the strength of materials shear shape factor of the section and $r^2 = I/A$.

The nth mode of vibration of the simply supported beam, (i.e. satisfying (4.2)) is given by:

$$w_n(x,t) = A_n \sin\frac{n\pi x}{\ell}\, e^{\imath\hat{\omega}_n t} \tag{4.7}$$

where $\hat{\omega}_n$ is a solution of the complex frequency equation:

$$c^2\alpha_n^4 - [1+\alpha_n^2 r^2(1 + \frac{k\tilde{E}_A}{\tilde{G}_A})\hat{\omega}_n^2 + \frac{kr^2\rho}{\tilde{G}_A}\hat{\omega}_n^4 = 0 \quad \text{(a)}$$

$$\alpha_n = \frac{n\pi}{\ell} \quad \text{(b)} \tag{4.8}$$

The solution of (4.8) is the complex "frequency"

$$\hat{\omega}_n = \hat{\omega}_n^R + \imath\hat{\omega}_n^I \tag{4.9}$$

In the case of small loss tangents of order (2.6) it can be shown by straightforward calculations that:

$$c^{R^2}\alpha_n^4 - [1+\alpha_n^2 r^2(1 + \frac{kE_A^R}{G_A^R})]\hat{\omega}_n^{R^2} + \frac{kr^2\rho}{G_A^R}\hat{\omega}_n^{R^4} = 0 \quad \text{(a)}$$

$$c^{R^2} = \frac{E_A^R I}{\rho A} \quad \text{(b)} \tag{4.10}$$

$$\hat{\omega}_n^I = \frac{\hat{\omega}_n^R}{2}\,\frac{(\hat{\omega}_n^R\, kr^2\rho/G_A^R - \alpha_n^2 r^2 kE_A^R/G_A^R)\tan\delta_G - (c^{R^2}\alpha_n^2/\hat{\omega}_n^{R^2})\tan\delta_E}{2\hat{\omega}_n^{R^2} kr^2\rho/G_A^R - [1+\alpha_n^2\gamma^2(1+kE_A^R/G_A^R)]} \tag{4.11}$$

It is seen that (4.10) is the frequency equation of an elastic Timoshenko beam in terms of real parts of complex moduli. Its validity is based on the usual additional assumption that real parts of complex moduli vary sufficiently slowly with frequency. Once $\hat{\omega}_n^R$ has been computed from (4.10), $\hat{\omega}_n^I$ can be computed from (4.11).

A mostly sufficient accurate approximation for $\hat{\omega}_n^R$ is:

$$\hat{\omega}_n^R \cong c^R\alpha_n^2\left[1 - \frac{1}{2}\alpha_n^2 r^2\left(1 + \frac{kE_A^R}{G_A^R}\right)\right] \tag{4.12}$$

For slender beams and low modes the first term in each of numerator and and denominator of (4.11) is insignificant relative to the others. Thus:

$$\hat{\omega}_n^I \cong \frac{(\alpha_n^2 r^2 kE_A^R/G_A^R)\tan\delta_G + (c^{R^2}\alpha_n^4/\hat{\omega}_n^{R^2})\tan\delta_E}{1 + \alpha_n^2 r^2\,(1 + kE_A^R/G_A^R)} \tag{4.13}$$

Substitution of (4.9) into (4.7) results in:

$$w_n(x,t) = A_n \sin\frac{n\pi x}{\ell}\, e^{-\hat{\omega}_n^I t}\, e^{\imath\hat{\omega}_n^R t} \tag{4.14}$$

where the attenuation is now:

$$\hat{\eta}_n = \hat{\omega}_n^I \tag{4.15}$$

To obtain an idea of the relative importance of damping due to shear and rotatory inertia, the attenuations (4.5) and (4.15) have been compared for the following case: Beam of rectangular section

$$\ell = 40.0" \qquad h = 2.0"$$

Material: Boron fibers, Epoxy matrix

$$v_f = v_m = .5$$

$E_f = 60\times10^6$psi, $E_m^R = .5\times10^6$psi, $G_m^R = .185\times10^6$psi

$$\tan\delta_E^m = \tan\delta_G^m = \tan\delta^m = .05$$

$$E_A^R = 30.25\times10^6\text{psi} \qquad G_A^R = .544\times10^6\text{psi}$$

$$\tan\delta_E = \frac{\tan\delta_m}{120} \qquad \tan\delta_G = \tan\delta_m$$

$$\rho = 1.78\times10^{-4}\ \text{lb(mass)/in}^3$$

It has been assumed for simplicity that real parts of complex moduli and loss tangents are frequency independent.

For the first mode:

$\omega_1^R = 1480$ 1/sec
$\eta_1 = .308$ 1/sec } Bending only

$\hat{\omega}_1^R = 1380$ 1/sec
$\hat{\eta}_1 = 4.44$ 1/sec } Timoshenko beam

It is seen that shear and rotatory inertia have a very small effect on the frequency but increase the attenuation by a factor of 14.4. This example shows that for damping of viscoelastic fiber reinforced beams shear and rotatory inertia are of major importance.

4.2 Forced torsional vibrations of laminated cylinder.

A thin walled cylinder which is laminated through its thickness is built in at one edge and is subjected to a sinusoidal forcing torque at its other edge. Each lamina is uniaxially reinforced and has the same material properties with respect to its material axes. The laminate is symmetric with following lamination scheme:

reinforcement in generator direction (axial) - volume fraction v_o

reinforcement in + θ direction - volume fraction v_θ

reinforcement in - θ direction - volume fraction $v_{-\theta}$

$$v_\theta = v_{-\theta} \tag{4.16}$$

For the purpose of analysis of torsional vibrations, the only effective laminate property needed is the effective complex shear modulus $\tilde{G}^*_{12}$. It follows from (3.11) that:

$$\tilde{G}^*_{12} = \tilde{C}^*_{1212} = {}^{(o)}\tilde{C}_{1212}t_o/h + {}^{(+\theta)}\tilde{C}_{1212}t_{+\theta}/h + {}^{(-\theta)}C_{1212}t_{-\theta}/h \tag{4.17}$$

where t_o is the sum of the thickness of the θ=0 laminae, $t_{+\theta}$ and $t_{-\theta}$ - the sums of the thicknesses of the $+\theta$ and $-\theta$ laminae, respectively.

Now:

$$t_o/h = v_o$$
$$t_{+\theta}/h = t_{-\theta}/h = v_\theta \tag{4.18}$$

and from the last of (3.16)

$${}^{(+\theta)}\tilde{C}_{1212} = {}^{(-\theta)}\tilde{C}_{1212} = {}^{(\theta)}\tilde{C}_{1212} = {}^{(\theta)}\tilde{C}_{44} \tag{4.19}$$

Introduction of (4.18-19) into (4.17) yields

$$\tilde{G}^*_{12} = {}^{(o)}\tilde{C}_{44}v_o + 2{}^{(\theta)}\tilde{C}_{44}v_\theta \tag{4.20}$$

By the last of (3.16) and from (2.4),(4.20) assumes the form:

$$\tilde{G}^*_{12} = \tilde{G}_A v_o + [\tfrac{1}{2}(\tilde{n}+\tilde{k}-2\tilde{\ell}+\tilde{G}_T)\sin^2 2\theta + 2\tilde{G}_A\cos^2 2\theta]v_\theta \tag{4.21}$$

It has been mentioned before (Section 2) that the imaginary parts of $\tilde{n}$, $\tilde{\ell}$ and $\tilde{k}$ can be neglected with respect to the imaginary parts of $\tilde{G}_T$ and $\tilde{G}_A$ for the usual fiber reinforced material. Consequently, the separation of (4.21) into real and imaginary parts assumes the form:

$$G^{*R}_{12} = G^R_A v_o + [\tfrac{1}{2}(n^R+k^R-2\ell^R+G^R_T)\sin^2 2\theta + 2G^R_A\cos^2 2\theta]v_\theta \tag{a}$$

(4.22)

$$G^{*I}_{12} = G^I_A v_o + (\tfrac{1}{2}G^I_T\sin^2 2\theta + 2G^I_A\cos^2 2\theta)v_\theta \tag{b}$$

In the usual fiber reinforced materials generally

$$\tfrac{1}{2}(n^R+k^R-2\ell^R+G^R_T) > 2G^R_A$$

$$\tfrac{1}{2}G^I_T < 2G^I_A$$

It follows that the shear loss tangent of the laminate

$$\tan\delta^* = \frac{G^{*I}_{12}}{G^{*R}_{12}} \tag{4.23}$$

has a maximum for θ=0 and decreases monotonically to a minimum for θ=45°. On the other hand shear strength is smallest for θ=0 and increases monotonically to a maximum for θ=45°. Therefore, in design for maximum damping it is necessary to choose the smallest angle θ which complies with allowable shear stress.

Let the forcing torque at the edge $x_1=\ell$ be represented as

$$M = M_o\sin\omega t$$

and let the amplitude of angle of twist ϕ at $x_1=\ell$ be written Amp (ϕ). By standard theory of viscoelastic vibrations with small loss tangents[2,3]

$$\text{Amp}(\phi) = \frac{cM_o}{JG^{*R}_\omega}\frac{\sqrt{\sin^2(2\alpha)+\sinh^2(2\beta)}}{\cos 2\alpha + \cosh(2\beta)} \tag{4.24}$$

where

$c^2 = \dfrac{G^{*R}_{12}C}{\rho I}$

$\alpha = \dfrac{\omega\ell}{c}$

$\beta = \dfrac{\omega\ell\delta^*}{2c}$

ρ - density

C - Torsional constant of section

J - Polar moment of inertia of section

G^{*R}_{12} - equ. (4.22a)

δ^* - equ. (4.23)

Numerical analysis has been carried out for a laminate composed of boron/epoxy laminae with both constituent volume fractions equal to .5. Laminae fractional volumes in laminate are

$v_o = .6$ $v_{\pm\theta} = .2$ with $\theta = 22.50°$

Analysis has been performed in following stages

(a) Experimental results for epoxy matrix complex shear modulus and loss tangent as a function of frequency have been described by an empirical formula.

(b) This formula together with elastic properties of fibers have been used to compute effective complex moduli of the uniaxially reinforced laminae, as a function of frequency. For this purpose results (2.7-9) and other formulae given in (2,3)have been used.

(c) With the aid of single laminae properties the real and imaginary parts (4.22) of the effective complex shear modulus G^*_{12} have been computed as function of frequency. It should be noted that in the present application: 1 indicates generator direction of cylinder, and 2 the direction normal to generator and tangent to section contour.

(d) The results for G^{*R}_{12} and G^{*I}_{12} have been used to compute (4.24) as a function of frequency ω.

A plot of such results is shown in Fig. 3 for a cylinder of length ℓ=100 in. and thin walled circular section. It is seen that the first resonance peak is very significant and may be regarded as an elastic resonance. However, the damping of the viscoelastic matrix becomes more effective with higher order resonanees, the fourth one being considerably reduced.

5. Conclusion

It has been shown that complex moduli of uniaxially fiber reinforced materials and of laminates of such materials, consisting of viscoelastic matrix and elastic fibers can be computed in straight forward fashion. The results can be used for analysis of structural vibrations on the basis of available theory.

Two structural examples have been given to assess the significance of vibration damping.

Many more other interesting applications can be analyzed by the theory which has been presented.

References

(1) Z. Hashin - "Complex moduli of viscoelastic composites - I. General theory and application to particulate composites" Int. J. Solids Structures 6, 539-552, (1970).

(2) Z. Hashin - "Complex moduli of viscoelastic composites - II. Fiber reinforced materials" Int. J. Solids Structures 6, 797-807, (1970).

(3) Z. Hashin - "Theory of fiber reinforced materials" Pt. 4, Final Report. Contract NAS 1-8818 NASA, Langley Research Center, Nov. (1970). NASA CR-1974 (1972)

(4) Y. Stavsky - "Bending and stretching of laminated aelotropic plates" Trans. ASCE, EM Div. 127, Pt. I, 1194-1219, (1962).

(5) R. M. Christensen - Theory of Viscoelasticity - Academic Press, (1971).

(6) W. Nowacki - Dynamics of Elastic Systems - Chapman & Hall, (1963).

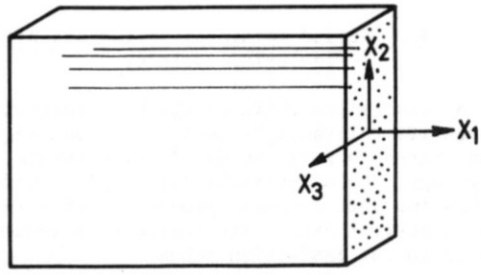

FIG. 1 UNIAXIALLY FIBER REINFORCED MATERIAL

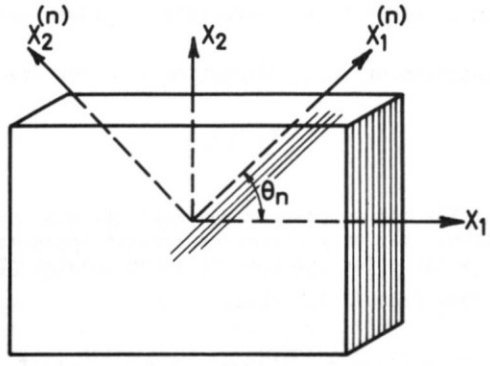

FIG. 2 LAMINATE

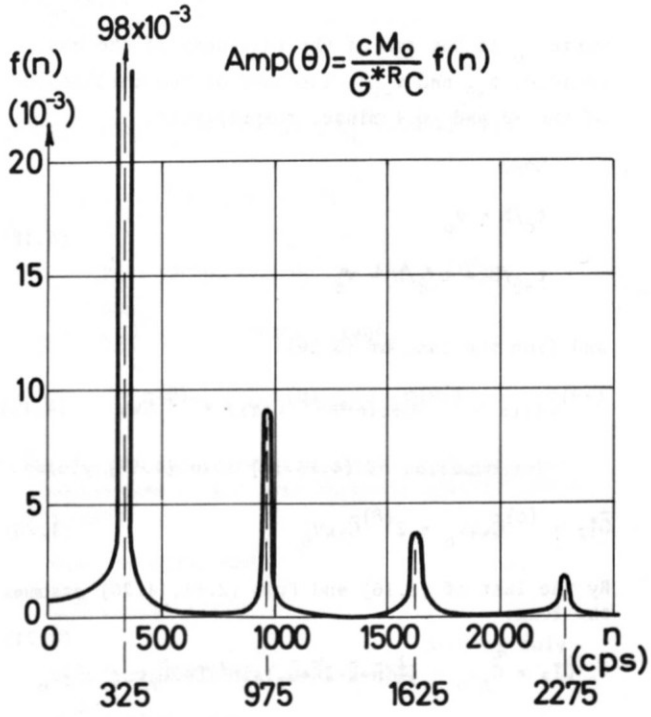

FIG. 3 AMPLITUDE OF ANGLE OF TWIST

DYNAMIC INELASTIC PROPERTIES OF MATERIALS

Part II - Representation of Time Dependent Characteristics of Metals(*)

S.R. Bodner and Y. Partom
Department of Materials Engineering
Technion - Israel Institute of Technology
Haifa, Israel

Abstract

A new approach to the representation of time dependent inelastic material behavior is described. Realistic properties such as strain hardening, strain rate effects, and anelasticity can be incorporated in this description which is particularly well suited for the computational solution of structural problems involving cyclic loading and large inelastic strains. Application to technological metals such as titanium is indicated.

1. Introduction

The analysis of the mechanical response of structures and machine parts in the range where the material response is inelastic and time dependent requires adequate representation of the material behavior under those conditions. The classical idealizations of elasticity, plasticity, and viscoelasticity have considerable limitations when time effects combined with strain hardening and inelasticity are significant factors. These limitations are especially severe when the structures are subjected to complicated loading histories that include changes of direction and rate of loading such as cyclic loading in the inelastic range. The various generalizations of the classical material idealizations that have been proposed to account for certain material properties, e.g. rate dependent plasticity, [1,2], are difficult to use in structural problems and do not properly represent material response for general loading and unloading histories.

The present paper reports on a new method of characterization of material behavior that can serve for a wide range of properties including strain hardening, strain rate sensitivity, anelasticity, accumulation of large plastic strains, and creep. The method is well suited for the computer solution of structural problems involving large deformations and complicated loading histories. An interesting aspect of the representation is that the stress strain curve of the material is a consequence of the constitutive equations and the conditions of loading. That is the stress strain curve is the solution of a particular boundary value problem and is not a "basic" material property.

A description of this approach has appeared in an earlier paper[3] for the case of perfect plasticity, i.e. neglect of strain hardening. The present paper reviews the procedure including the consideration of strain hardening. Examples are given to show the applicability of the equations to the case of titanium tensile specimens subjected to uniaxial loading at various uniform and changing strain rates.

2. General Formulation

The essential point of the present procedure is that the deformation rate tensor d_{ij} is considered to consist of both elastic (fully reversible) and inelastic (irreversible) components at each stage,

$$d_{ij} = d^e_{ij} + d^p_{ij} \tag{1}$$

The relations between these components and the elastic stress, which is the reference state variable, are the basic constitutive equations of the material. There is therefore no distinct region of material response that is fully elastic since inelastic strains would be present at all stages of loading and unloading. A special unloading criterion is therefore not required since the same constitutive equations hold under all conditions. This makes the method particularly well adopted for computer applications involving arbitrary loading histories.

Another consideration is that the total stress contains an anelastic component in addition to the elastic stress. The anelastic stress is introduced to account for viscous resistance to motion and is responsible for energy losses for geometrically reversible motions, e.g. internal damping. This stress can, in general, be expressed as a function of the elastic stress and the total deformation rate. The anelastic stress will, however, be taken as zero in the examples discussed in this paper.

The equations relating the deformation rate to the velocity gradients and the strain rate using the Almansi strain measure have been described for general deformation states[3]. The elastic strain is a function of the elastic stress, so the elastic component of the deformation rate can, upon integration, be directly related to the elastic stress.

The constitutive law for the plastic (irreversible) component is also a relation between d^p_{ij} and σ_{ij}. In the following the flow law of classical plasticity, this relation is taken to have the general form

$$d^p_{ij} = \overset{\circ}{d}{}^p_{ij} = \lambda \sigma_{ij} \tag{2}$$

(*) The research reported in this paper has been sponsored in part by the Air Force Office of Scientific Research through the European Office of Aerospace Research, OAR, United States Air Force under Contract F 44620-72-C-0004.

where the bar symbol refers to the deviatoric tensor. The quantity λ is determined by squaring (2) to give

$$\lambda^2 = \underline{D}_2^p / \underline{J}_2 \tag{3}$$

where $\underline{J}_2$ is the second invariant of the elastic stress deviator and $\underline{D}_2^p$ is the second invariant of the plastic deformation rate tensor. The von Mises yield criterion of classical plasticity states that plastic flow occurs when, in the present notation,

$$\underline{J}_2 = - Y^2/3 \tag{4}$$

where Y is the yield stress in tension.

The present viscoplastic theory considers that a relation exists between $\underline{D}_2^p$ and $\underline{J}_2$ to be used in conjunction with (2) and (3). This relation between the plastic deformation rate and the elastic stress invariants,

$$\underline{D}_2^p = f(\underline{J}_2) \tag{5}$$

therefore forms the constitutive equation for describing the viscoplastic deformation properties of the material. Expressions for this relation are motivated by the equations relating dislocation velocity with stress which are basic to the field of "dislocation dynamics," e.g.[4] A useful particular form for (5) is

$$D_2^p = D_o^2 \exp\left(-[C^2/(-\underline{J}_2)]^n\right) \tag{6}$$

where

$$C^2 = \frac{1}{3} Z^2 \left(\frac{n+1}{n}\right)^{1/n} \tag{6a}$$

In these equations, D_o, Z and n are material parameters. The coefficient D_o is the asymptotic value of the deformation rate at large stresses, i.e. the plastic deformation rate is bounded. The quantity n is a measure of the steepness of the curve and is therefore a measure of the strain rate sensitivity of the material; larger values of n would correspond to a steeper slope and therefore mean the response is less rate sensitive. The parameter Z is related in a very general way to the yield strength of the material since the maximum slope of the curve occurs when

$$\underline{J}_2 = -Z^2/3 \tag{7}$$

However, there is no direct correspondence between Z and the usual definitions of yield stress.

To incorporate strain hardening into the formulation it is necessary to identify the variables that represent this property. The simplest and seemingly most logical is the work done during plastic deformation, W_p, since all strain hardening mechanisms described in the metallurgical literature depend in some manner on this parameter. This had also been suggested by Hill[5] as the most significant single factor for strain hardening. On the microscopic level, strain hardening means increased resistance to dislocation motion and therefore to plastic flow. In the present formation this would correspond to d_{ij}^p being a decreasing function of W_p which is a state variable. There should, however, be a limiting lower limit to d_{ij}^p since otherwise the material would behave fully elastically as W_p became very large. That would correspond to an upward turning on the stress strain curve at large strains which is not realistic. Microscopic analyses also indicate that plastic flow never fully ceases since there are limits to the distances between the obstacles that oppose dislocation motion. Strain hardening can therefore be introduced into (6) by making D_o a decreasing function or C an increasing function of W_p. The latter was chose in the present example and the parameter Z was taken to have the form

$$Z = Z_1 + (Z_o - Z_1)\, e^{-mW_p/Z_o} \tag{8}$$

where Z_1, Z_o, and m are new material parameters.

This formulation of strain hardening corresponds to isotropic hardening which means that it would not account for any Bauschinger effect. That would require introducing particular non-symmetric features into the analysis which is possible in principle but very complicated. The above formulation could also account for other special material effects such as age hardening and strain ageing. Age hardening would mean that d_{ij}^p would be a decreasing function of absolute time. Strain ageing is a more complicated phenomenon and could be considered by making d_{ij}^p decrease with the time of deformation. This would mean that shorter deformation times would correspond to larger values of d_{ij}^p and therefore to lower stresses which are the macroscopic characteristics of strain ageing. The present example, however, considers only strain hardening as indicated by (8).

3. Specialization to Uniaxial Straining

The examples described in this paper are of uniaxial straining of a material at various uniform and changing strain rates. The constitutive equations developed for this case can also be used for multiaxial boundary value problems.

The deformation rate tensor is defined in terms of the velocity gradient,

$$d_{ij} = 1/2(v_{i,j} + v_{j,i}) \tag{9}$$

where v_i is the velocity vector. For the uniaxial stress state, the only non-zero deformation rate components are d_x (axial direction) and d_y in both transverse directions. All shearing components vanish for this case. The axial deformation rate is simply

$$d_x = \frac{dv_x}{dx} \tag{10}$$

where v_x is the particle velocity in the axial direction. In terms of the crosshead velocity of the straining device V_c and the specimen gauge length L,

$$d_x = V_c/L \tag{11}$$

The other component d_y is determined by the state of

stress. The deviatoric components of the deformation rate are then given by

$$\underset{-}{d}_x = 2/3\ (d_x - d_y) \tag{12a}$$

$$\underset{-}{d}_y = \underset{-}{d}_z = -\ 1/3\ (d_x - d_y) \tag{12b}$$

and each component is considered to be the sum of elastic and plastic parts, e.g.

$$\underset{-}{d}_x = \underset{-}{d}^e_x + \underset{-}{d}^p_x \tag{13}$$

The elastic stress-strain relations, assuming the elastic strains are sufficiently small so that Hooke's Law is applicable, are

$$\underset{-}{\sigma}_{ij} = 2G\ \underset{-}{\varepsilon}_{ij} \tag{14}$$

$$\sigma_{kk} = 3K\ \varepsilon_{kk} \tag{15}$$

and in this example σ_x is the only non-zero stress component.

For large strains, the deformation rate is not, in general, equal to the strain rate[3]. However, this identity does hold for the simple geometry of the present problem since the other terms in the general relationship become zero.

The elastic part of the deformation rate tensor is related to the stresses through (14) and (15) and the plastic part through (2), (3), (6) and (8). The material is compressible for elastic deformations (15) and is incompressible for plastic deformations in accordance with the flow law (2). The rate of plastic work, W_p, is given by

$$\dot{W}_p = \sigma_{x-x} d^p \tag{16}$$

These equations can then serve to determine the stress required to pull a rod of the material at a uniform velocity V_c. This is actually a particular boundary value problem whose solution leads to the uniaxial force-elongation (stress-strain) relation of the material.

A numerical scheme was devised to compute the stress from the preceding equations when the material constants and the applied velocity V_c are given. The method is a step by step procedure which follows the deformation history. All quantities such as d^e_{ij}, d^p_{ij}, W_p, the total elongation, and the stress are determined at each step. The numerical scheme can be readily adjusted to account for changes in the applied velocity and for loading and reloading. That is, the method can consider completely arbitrary loading or straining histories. In this paper, however, only examples involving uniform velocities and a single change of velocity are described.

4. Application to Titanium

A series of tensile tests were performed in a 10 ton capacity Instron testing machine on specimens of commercially pure titanium. The specimens were cut from a 1 mm thick plate in the rolling direction and were 8 mm wide. An extensometer was used for the strain measurement and the load was recorded as a function of strain. Titanium is a fairly rate sensitive material which makes it useful for studying the effect of different straining rates and the response to changes of rate during a test. In general, material response is influenced by the complete strain rate history and titanium appears to be a good specimen material for such studies. This has been emphasized recently by a number of investigators, e.g.[6]. The proposed method of material representation and the associated constitutive equations intrinsically include strain rate history effects.

In order to examine the applicability of the present theory to titanium, the material constants of the constitutive equations, (6), (6a), (8) were determined from the results of two tests at different constant extension rates. The response to other straining rates and to varying straining histories were then calculated and compared to corresponding experimental results.

Tests were conducted for four constant crosshead velocities: 0.005, 0.05, 0.5 and 1.0 cm/min. The effective overall specimen gauge length was 52 mm so the imposed velocities correspond respectively to the strain rates: 1.6×10^{-5}, 1.6×10^{-4}, 1.6×10^{-3}, and $3.2 \times 10^{-3}\ \text{sec}^{-1}$.

The material constants were obtained by fitting the calculated response of the material at the highest and lowest rates to the corresponding experimental curves. The values of the material constants determined in this manner for commercially pure titanium are:

$$Z_o = 11.5 \text{ Kbars } (112.8 \text{ Kg/mm}^2)$$

$$Z_1 = 14.0 \text{ Kbars } (137.0 \text{ Kg/mm}^2)$$

$$D_o^2 = 10^8 \text{ sec}^{-2}$$

$$n = 1$$

$$m = 100$$

The elastic constants for titanium are

$$K = 1.23 \times 10^3 \text{ Kbars } (12.0 \times 10^3 \text{ Kg/mm}^2)$$

$$G = 0.44 \times 10^3 \text{ Kbars } (4.3 \times 10^3 \text{ Kg/mm}^2)$$

The calculated load-elongation curves for these constants are shown in Fig. 1 for the highest and lowest straining rates. Also shown are the experimental curves to which they were fitted. Calculated load-elongation curves for the other straining rates are shown in Fig. 2 along with the corresponding experimental results.

Of greater interest is the effect of varying strain and strain rate histories on the deformation characteristics. One significant experiment of this kind is to change the crosshead velocity during the course of a test. This can be easily accomplished on an Instron machine by pressing the button that activates a magnetic clutch on the speed regulator. A number of tests were run in which the slowest and fastest rates were interchanged at 4% strain without unloading. The experimental results were consistently reproducible, Figs. 3, 4, and could be summarized as follows:

(a) Immediately upon changing from the high to the low rate, the stress drops in an essentially

elastic manner to about or slightly above the level corresponding to the lower rate for a constant rate test. The stress then shows a small rise and continues approximately parallel and above the constant rate curve and tends toward it with increasing strain (Fig. 3).

(b) Upon changing from a lower to a higher rate, the immediate response is close to the elastic value and the stress then approaches the curve corresponding to the higher uniform rate test but at a lower level. There is a small rise and fall of the stress curve after the initial elastic response which is similar to the "upper yield point" phenomena. The stress tends toward the uniform rate curve with increasing strain. The flow stress at a high rate is therefore less when it is subjected to prior deformation at a low rate than if uniformly strained at the high rate (Fig. 4).

Another closely related experiment would be to unload the specimen at a given strain and then to reload at a different rate. A few experiments of this kind were performed and the results indicated little overall difference between this case and that of rate changing without unloading. The "cusp" observed in going from the high to the low rate in the former tests is not observed when the specimen is fully unloaded before the rate is changed. An "upper yield point" effect is also observed in this case upon reloading at a higher rate, but it is less pronounced than when the rate is changed without unloading.

Similar experiments to type (b) above, namely changing from a low to a high rate without unloading have been performed on titanium in shear[6] with generally similar results. The "upper yield point" effect was, however, not observed in those tests[6]. An experiment of this kind on aluminum for a very large change of rate of loading has been reported[7] and the "upper yield point" behavior of the incremental response was observed. Various experiments on changing the rate of straining after complete unloading were performed on aluminum[8,9] and led, in general, to results similar to those obtained here.

The calculated response of the material based on the present theoretical formulation for the same variable strain rate history gave results that closely approximated the experimental ones, Figs. 3, 4. The "cusps" observed on reducing the strain rate and the "upper yield point" observed on increasing the rate were, however, not reproduced in the calculated response curves. These seem to be transient effects which depend on more detailed mechanisms of plastic flow than are represented in the present theoretical formulation. It may be possible to include such effects by generalizing the material constants to more closely simulate microscopic parameters (internal variables) such as dislocation density and velocity. The reason for the respective stress levels upon changing rates can be explained in terms of the plastic work W_p prior to the rate change which influences the subsequent flow stress. W_p is larger at the higher rate which leads to a relatively higher stress curve upon reducing the rate (compared to a constant lower rate test), while the reverse holds for the other case. These stress level differences could also be explained in terms of the developed microstructure but this will be left to a subsequent paper.

It is particularly interesting to examine the details of the deformation upon changing from the lower to the higher rate. For this particular case, the plastic deformation rate component d^p_{ij} is initially 99.7% of the total d_{ij}. Immediately after the change the value of d^p_{ij} increases slightly but its percentage of d_{ij} drops to 56.6%.

The incremental response is largely elastic and experimentally may appear to be fully elastic for approximate measurements. If the change of imposed velocity at the specimen end had been sufficiently rapid to generate waves, then an elastic wave would propagate along the specimen. The plastic component would not be dominant and would attenuate rapidly with distance. Observations some distance from the end would indicate that the incremental response to the velocity change is elastic.

The proposed constitutive equations are also suitable for cyclic loading histories, which would be important for low cycle fatigue studies. An independent criterion, however, would have to be introduced to indicate the onset of fatigue microcracks or other failure phenomena. If such a criterion were expressible in terms of the state variables σ_x and W_p, then the present analysis could serve to determine the condition for which the criterion would be reached for very general cyclic loading histories.

REFERENCES

1. Malvern, L.E., "The Propagation of Longitudinal Waves of Plastic Deformation in a Bar of Material Exhibiting a Strain Rate Effect," Journal of Applied Mechanics, vol. 18, 1951, p. 203.
2. Bodner, S.R. and Symonds, P.S., "Experimental and Theoretical Investigation of the Plastic Deformation of Cantilever Beams Subjected to Impulsive Loading", Journal of Applied Mechanics, vol. 29, 1962, p. 719.
3. Bodner, S.R. and Partom, Y., "A Large Deformation Elastic-Viscoplastic Analysis of a Thick Walled Spherical Shell," Journal of Applied Mechanics, vol. 39, 1972.
4. Gilman, J.J., Micromechanics of Flow in Solids, McGraw-Hill, New York, 1969.
5. Hill, R., The Mathematical Theory of Plasticity, Clarendon Press, Oxford, 1950.
6. Nicholas, T. and Whitmore, J.N., "The Effects of Strain-Rate and Strain-Rate History on the Mechanical Properties of Several Metals," Report No. AFML-TR-70-218, Air Force Materials Lab., Wright-Patterson AFB, Ohio, August,1970.
7. Frantz, R.A. and Duffy, T., "The Dynamic Stress-Strain Behavior in Torsion of 1100-0 Aluminum Subjected to a Sharp Increase in Strain Rate," Journal of Applied Mechanics (to appear).
8. Lindholm, U.S., "Some Experiments with the Split Hopkinson Pressure Bar," J. Mech. Phys. Solids, vol. 12, 1964, p. 317.
9. Klepaczko, J., "Strain Rate History Effects for Polycrystalline Aluminium and Theory of Intersections," J. Mech. Phys. Solids, vol. 16, 1968, p. 255.

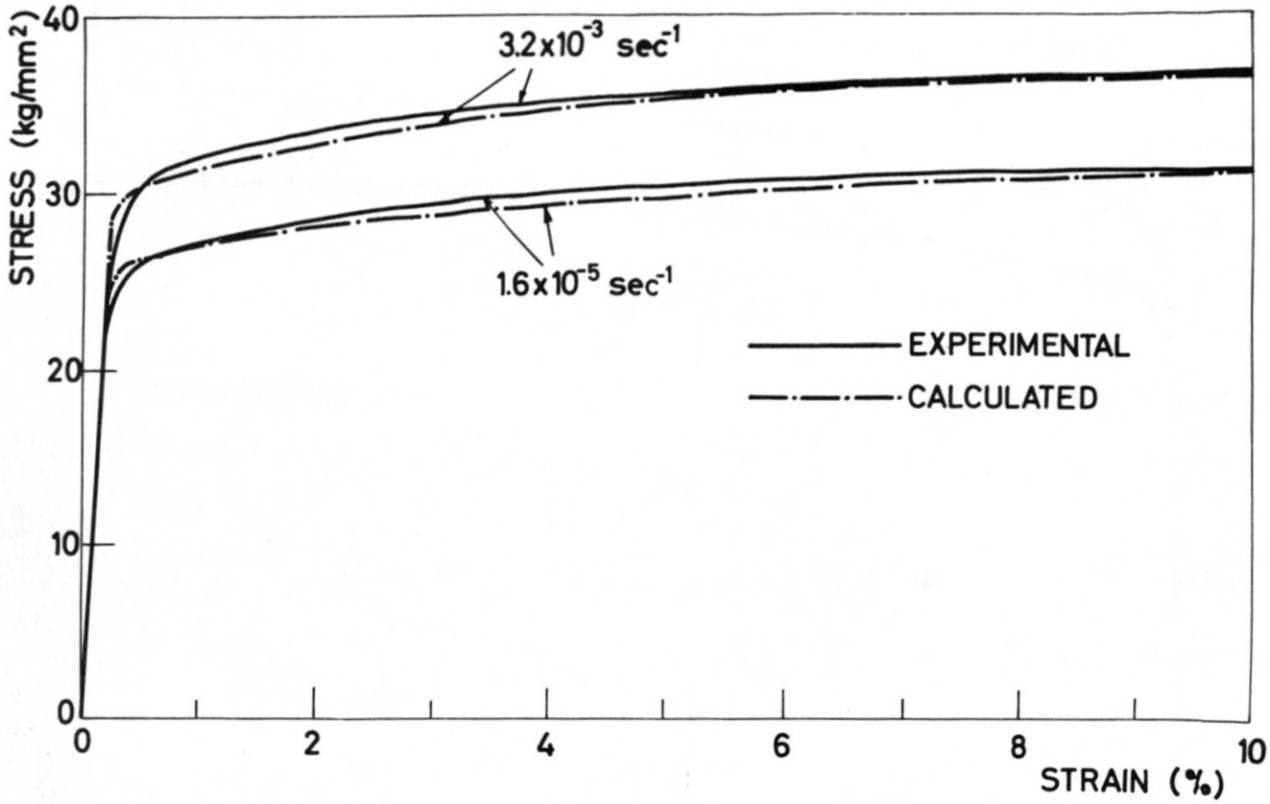

Fig. 1 - EXPERIMENTAL AND CALCULATED (FITTED) STRESS STRAIN CURVES FOR TITANIUM AT CONSTANT STRAIN RATES.

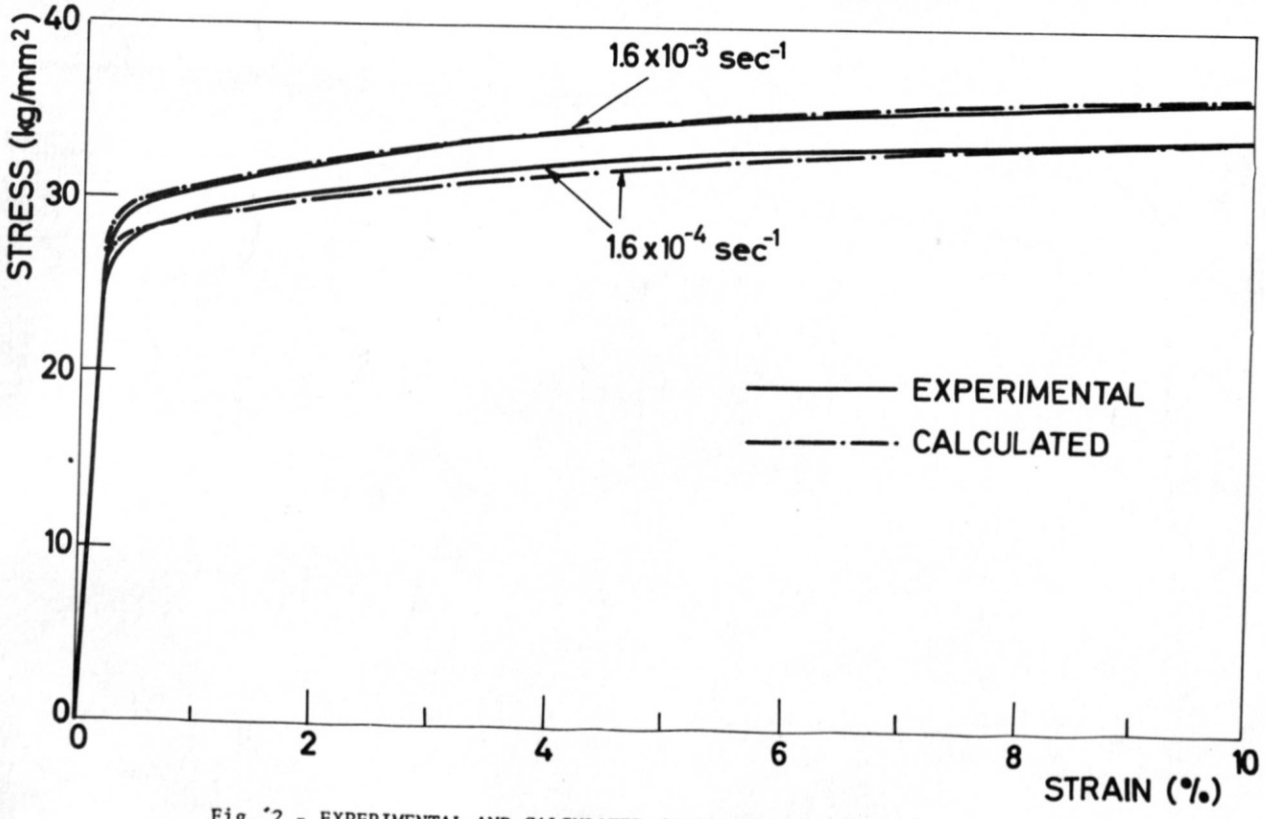

Fig. 2 - EXPERIMENTAL AND CALCULATED (DERIVED) STRESS STRAIN CURVES FOR TITANIUM AT CONSTANT STRAIN RATES.

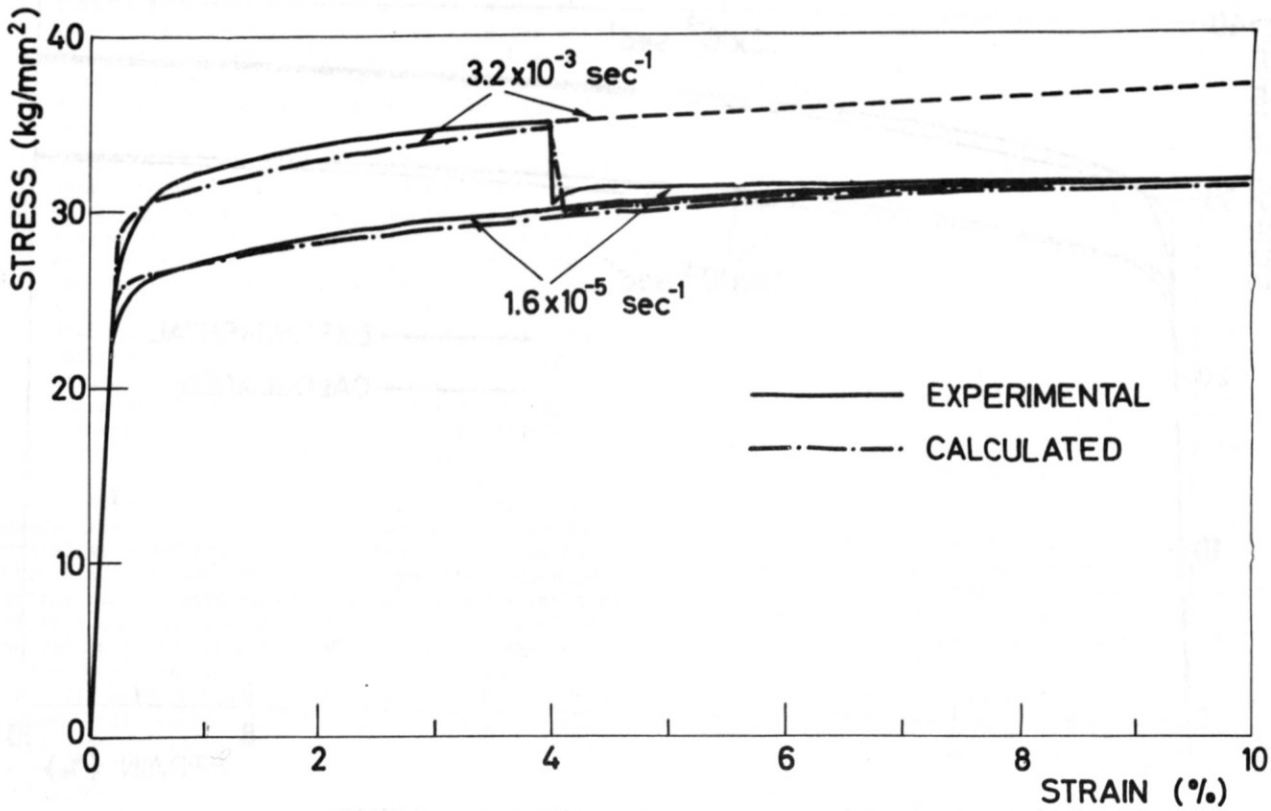

Fig. 3 - EXPERIMENTAL AND CALCULATED (DERIVED) STRESS STRAIN CURVES FOR TITANIUM SUBJECTED TO A RAPID CHANGE (DECREASE) IN STRAIN RATE.

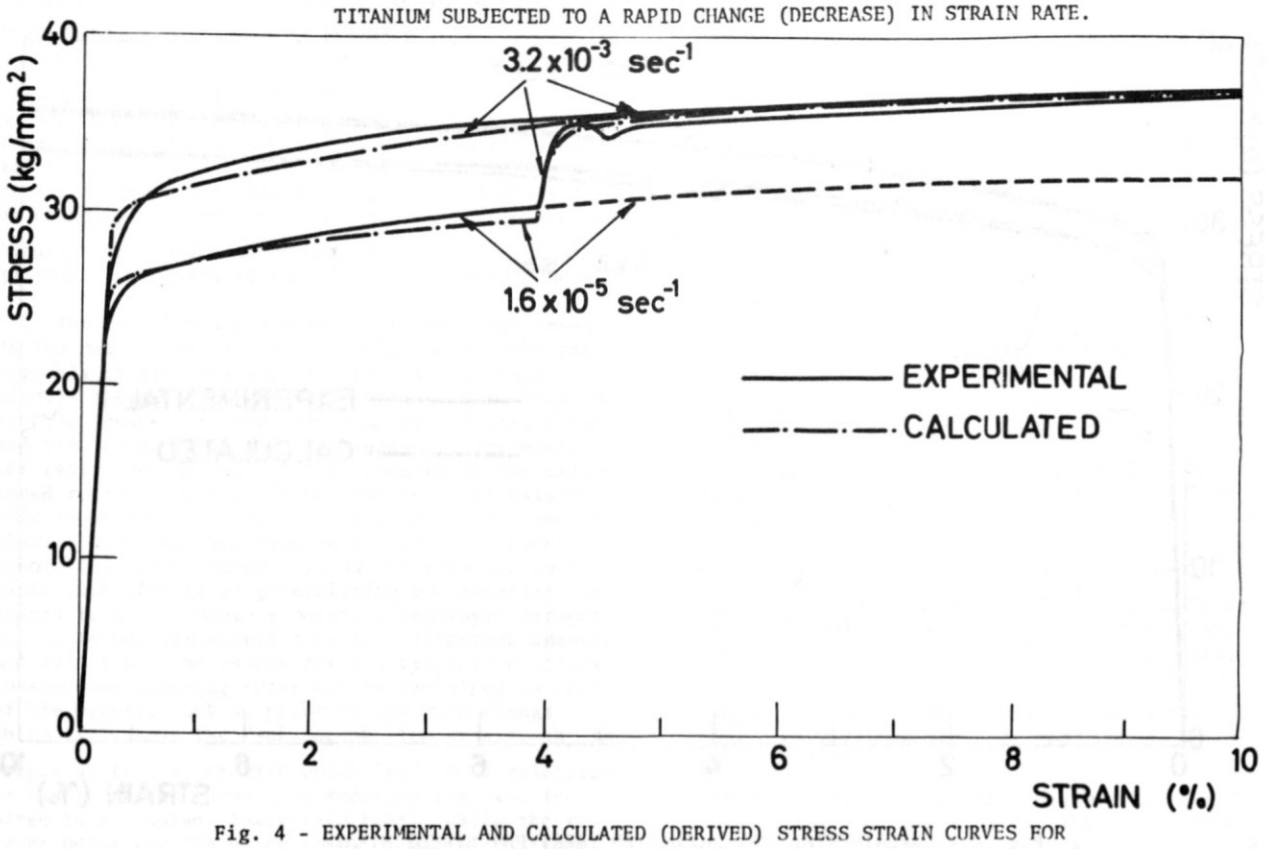

Fig. 4 - EXPERIMENTAL AND CALCULATED (DERIVED) STRESS STRAIN CURVES FOR TITANIUM SUBJECTED TO A RAPID CHANGE (INCREASE) IN STRAIN RATE.